JOURNAL OF SPACECRAFT AND ROCKETS
Vol. 30, No. 5, September–October 1993

Preliminary Structural Evaluation and Design of the HL-20

Lance B. Bush*
NASA Langley Research Center, Hampton, Virginia 23681
James C. Robinson†
Old Dominion University Research Foundation, Norfolk, Virginia 23508
and
Deborah M. Wahls*
NASA Langley Research Center, Hampton, Virginia 23681

A lifting body concept, the HL-20, was designed at NASA Langley Research Center, and a structural analysis of the configuration with a cylindrical pressurized crew cabin was presented. Loads for the vehicle were assembled from mission loading conditions such as abort, on-orbit pressurization, blast overpressure, aerodynamic maneuver, and touchdown. The critical loading conditions were identified, and resultant loads were mapped onto the structure in order to review the effects of the mission loading conditions. The HL-20 structural concept was sized for the mission loads, and the resulting structural weights were calculated.

Introduction

IN response to the personnel transport needs of the Space Station Freedom (SSF) and the need for assured manned access to space, candidate Personnel Launch System (PLS) concepts are currently under design and evaluation. The HL-20, a PLS concept, has been under study at the NASA Langley Research Center for several years.

This paper documents the structural design and analysis study of the reference structural concept for the HL-20. The structural analysis was performed using a finite element modeling and analysis method. The structural element sizing was performed with a fully stressed design sizing code plus satisfaction of overall buckling criteria. The structural concept is based on a cylindrical pressurized shell that serves as the crew compartment and the main structural load-bearing member. Analysis of a previous structural concept, featuring a pressure shell that conforms to the vehicle exterior shape, is documented in Ref. 1. The present study includes a definition of the structural configuration and identification of the mission loading conditions. The configuration is analyzed for structural integrity when subjected to the mission loading conditions. All structural elements are checked for failure due to the loading and are resized, where necessary, in order to obtain a safe structural configuration. The weight of the sized structural configuration is calculated, including a 50% increase for non-optimum considerations, thereby obtaining an analytically derived value as compared to the initial engineering estimate which was based on historical weight data and regression analysis.

Study Guidelines

The objectives for a PLS are low design and development costs and low cost-per-flight that are compatible with a safe, reliable, and easily maintainable and operable vehicle. The primary mission is the personnel transport to and from the SSF. Critical loading conditions affecting the vehicle structure are derived from this mission model. These conditions include ascent, abort from the pad, aerodynamic maneuver, and runway bump (Fig. 1). Thus, the structural configuration of the vehicle must be capable of withstanding failure due to the loading conditions of the mission model. The resulting weight of the vehicle must be approximately less than 10% of the total mass of the HL-20 vehicle to meet the performance requirements.

Vehicle Definition

Ground rules for the PLS study specify that the vehicle be designed for low operations and maintenance cost. Aircraft-type operations and maintenance were adopted in order to achieve quick turnaround times and efficient handling of the HL-20. The structural design and subsystem packaging of the HL-20 configuration were impacted greatly by these ground rules.[2]

Early designs for SSF called for an eight-member crew. Thus, the HL-20 vehicle was designed for a pilot, copilot, and eight passengers to support the design reference mission of SSF personnel change-out. The configuration has a length of 28.25 ft and a wing tip-to-tip width of 22.5 ft. The HL-20 structure is composed of two primary components: the crew

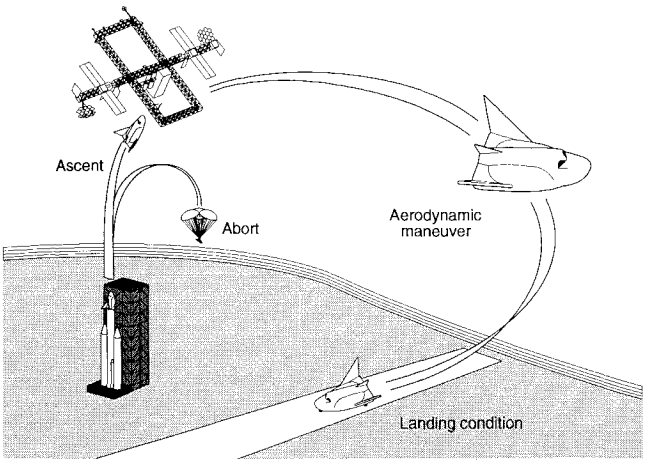

Fig. 1 Critical loading conditions.

Received Dec. 22, 1992; revision received Jan. 22, 1993; accepted for publication Jan. 29, 1993.

*Aerospace Engineer, Space Systems Division, Vehicle Analysis Branch. Member AIAA.
†Structural Engineer. Associate Fellow AIAA.

compartment and the heatshield (Fig. 2). The secondary structure consists of two canted fins or wings, eight large access panels, and a center fin which are not shown in Fig. 2. The crew compartment provides the necessary volume for crew habitability over the duration of the mission and serves as the primary structural element of the vehicle. The center section consists of a cylinder with a flat floor, a cockpit and close-out form the front, and a conical section form the aft end. Four frames extend from each side of the crew compartment to support the heatshield, subsystems, and the access panels. This crew compartment attaches to the booster at the aft end and supports all of the other components.

Entry and exit hatches are necessary for ingress and egress from the HL-20 while on the launch pad, during docking to the space station, on landing, and in the event of an emergency water-landing evacuation. The hatch located on the top of the vehicle can be used for prelaunch ingress and, in the case of a water landing, for egress. The aft hatch is for use in docking with the SSF and for normal egress on landing (Fig. 3).

The heatshield (Fig. 2) is suspended from the crew compartment by links to the extension frames and crew compartment. The heatshield provides thermal isolation from the crew compartment and, when removed, provides access to the pressure vessel during manufacturing and inspection. The heatshield is constructed of graphite polyimide honeycomb and employs a direct-bond thermal protection system (TPS) tile concept. Direct bonding of the tiles to a graphite polyimide structure with a similar coefficient of thermal expansion should result in less maintenance compared to the technique currently used on the Shuttle Orbiter which requires a strain isolation pad system.

In an effort to reduce recertification, refurbishment, and maintenance schedules, the HL-20 subsystems are positioned outside the crew compartment in a nonpressurized area (Fig. 4). This area is easily accessible through large access panels and contains the retractable landing gear, orbital maneuvering system (OMS), reaction control system, prime power, environmental control and life support system, avionics systems, and personnel provisions.

Structural Concept

The proposed structural concept for the HL-20 vehicle employs current technology materials and construction with the exception of a new approach for the lower surface TPS. The lower surface TPS consists of ceramic tiles direct bonded to a graphite polyimide honeycomb heatshield. The heatshield concept thus allows for a more streamlined operations and maintenance process. Direct application of the TPS to the vehicle structural skin is used on the remainder of the vehicle. High-density reusable surface insulation (HRSI) is employed on the lower surface heatshield and blankets and/or flexible reusable surface insulation (FRSI) on the upper surfaces (Fig. 5). Advanced carbon-carbon (ACC) is used in areas of high heating such as on the wing leading edge and control surface, nose, chines, and vehicle body flaps.

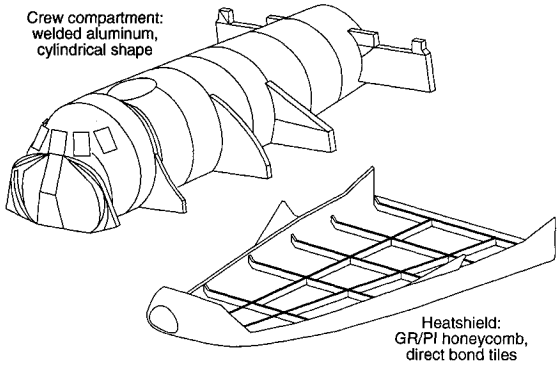

Fig. 2 Primary structures.

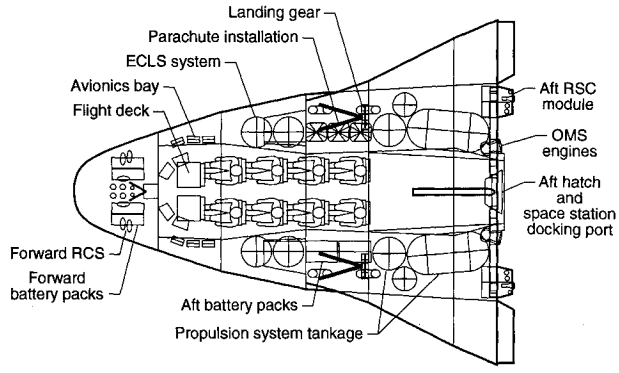

Fig. 3 HL-20 configuration.

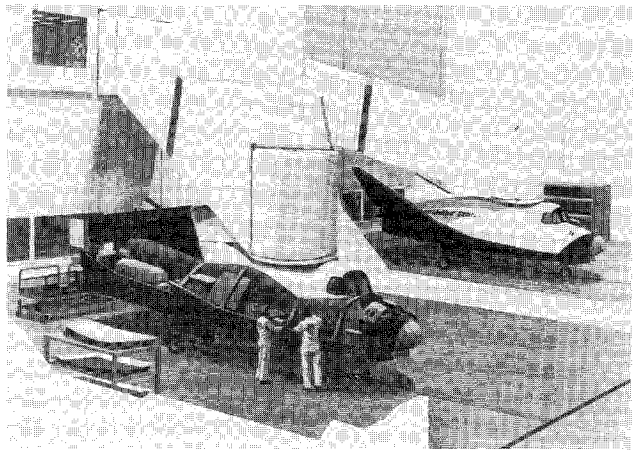

Fig. 4 HL-20 maintainability through subsystem access (courtesy of Rockwell International).

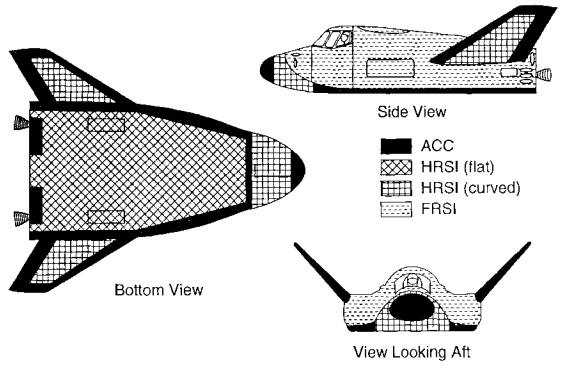

Fig. 5 HL-20 thermal protection system.

The crew compartment has an internal skin-stringer construction. Frames, also internal to the skin, are located approximately every 17 in. Aluminum 2219 is used for the crew compartment pressurized shell because of its relatively low cost, weldability, and historic performance. The crew compartment has welds and mechanical fasteners to insure sealing of the pressurized vessel. Within the crew compartment, a honeycomb floor is mounted on the primary ring frames. The honeycomb will consist of aluminum 2219 skin and an aluminum core. Subsystems are secured to the structure at the frame locations. Much of the forebody consists of a molded ACC nose cap similar in construction and installation to the Space Shuttle nose cap. The construction of the tunnel area is an aluminum 2219 skin-stringer configuration which is similar to that of the crew compartment.

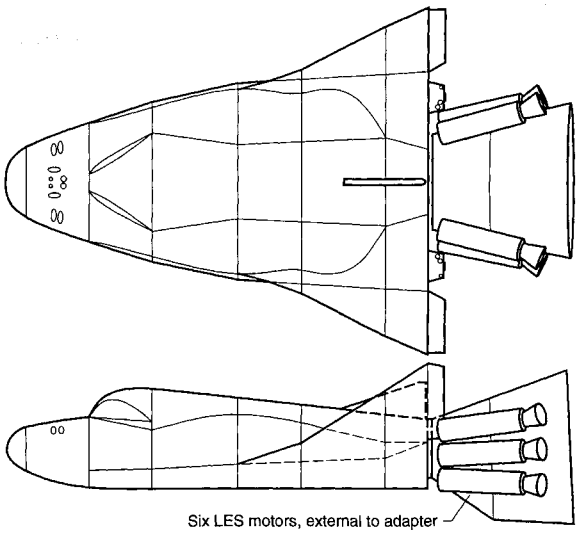

Fig. 6 Interface adaptor and abort motors.

Other significant structural components, besides the ring frames, are included in the internal arrangement of the vehicle. A forward and an aft bulkhead complete the crew compartment. Larger ring frames in the aft section of the vehicle serve to stiffen the body as well as provide a load path for the wing-spar-to-body intersection. In addition, points along the ring frames are used to attach the OMS. Four large axial beams serve as seat tracks and transmit the combined inertial load of personnel, suits, and seats to the reinforced tunnel area which serves as thrust structure. These axial beams also reduce vehicle flexure. Ribs and spars in the wing provide load paths into the body.

The surfaces of the vehicle are modeled using the physical properties of a skin-stringer and honeycomb construction. Bulkheads are modeled using plate properties with bar stiffeners while ring frames are modeled using membrane properties for webs and bar properties for the caps. Ribs and spar webs are modeled assuming membrane properties. All physical properties are initially set at a minimum practical manufacturing standard. Through sizing loops, these gauges are increased as needed to prevent failure or remain minimum gauge in cases of low loading.

Elements representing the subsystem masses are also included in the finite element model. These nonstructural elements are important because they introduce inertial forces into the structure when coupled with vehicle accelerations. Masses representing the subsystems (i.e., avionics, fuel tanks, etc.) are positioned within the structure consistent with the subsystem packaging arrangement in Fig. 4. In the case of personnel provisions, masses need to be calculated for the personnel, pressure suits, and seats. In accordance with the study guidelines, the HL-20 accommodates any personnel with stature ranging from a 5th percentile oriental female to a 95th percentile Caucasian male.[3] For a conservative mass representation, it is assumed that the crew and the passengers consist entirely of 95th percentile caucasian males.

Vehicle Loads

For this study, the SSF crew rotation mission is baselined for analysis and includes the following sequences: launch, ascent, orbit, docking, berthing, deorbit, descent, and landing. The design loading conditions for each mission phase are described in this section.

An on-the-pad or altitude abort yields a critical loading condition. To escape an explosion and its resulting overpressures, an 8-*g* acceleration is provided by the abort motors mounted on the HL-20 interface adaptor (Fig. 6). This axial acceleration is the maximum value expected for the vehicle during a normal mission or abort. At launch, all of the fuel and cargo are onboard, and this condition yields the maximum inertial forces on the vehicle. This condition is modeled by applying constraints at the interface adaptor/HL-20 attachment bolts, while the vehicle model and its associated subsystem masses are subjected to inertial loads equivalent to an 8-*g* acceleration. In addition, the overpressure from a booster explosion reaches approximately 10 psi on the exterior surfaces of the HL-20 and is modeled as such. Two loading cases are created, one with the overpressures and one without. In some cases, the abort maneuver may be executed without a blast overpressure occuring. In the case of an on-the-pad abort or abort up to 64 s after liftoff, the HL-20 has enough energy to return to the launch site. There are other abort landing sites available later in the trajectory, but a window exists between 64 s and 403 s where the vehicle must be aborted to a water landing aided by parachutes. Water impact loads could reach levels as high as 8 *g* due to the combined effects of vehicle impact and wave action.[4] Personnel safety is the primary concern in this case, while vehicle survivability is not a requirement. Parachutes are stored inside the access panels and are attached so that the aft end of the vehicle enters the water first. The parachutes slow the vehicle prior to water impact thereby reducing the impact load and the energy absorbed by the aft end of the vehicle. Quantification of the amount of structural damage allowed is beyond the scope of the present study. Therefore, an analysis of water impact is not presented.

The later phases of ascent present another design loading condition. Environmental compatibility with the SSF is a ground rule for this study. Thus, the crew compartment is designed for a 14.7-psi internal pressure. This absolute pressure causes a 14.7-psi differential across the crew compartment shell in space and at high altitudes. This pressurization is combined with a 3-*g* axial acceleration on ascent, as determined by trajectory analysis[5] to compose an additional critical loading condition.

Significant vehicle loads are not expected to occur during either docking or berthing. Some local loading will occur, but it is premature to estimate the loading when the hardware has yet to be defined.

Upon re-entry, aerodynamic effects become significant on the vehicle. The vehicle flies at an angle-of-attack ranging from 29 deg at hypersonic entry conditions to 5 deg at low supersonic speeds. The maximum dynamic pressure during this phase of entry occurs around Mach 2.5 where the flight angle of attack is 6 deg. At this condition, pressures on the wing are in the neighborhood of 3 psi. The most critical condition, the design condition, is an aerodynamic maneuver[6] with a 2.5-*g* acceleration normal to the vehicle.

A nominal landing sink rate of 3 ft/s is assumed. Performance analyses show that this sink rate is achievable for all

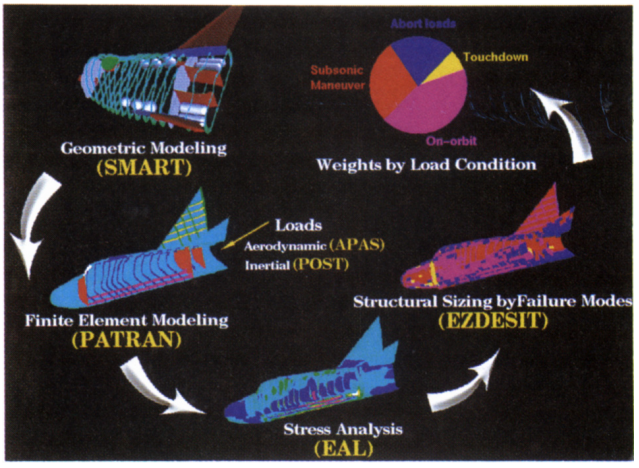

Fig. 7 Structural analysis methodology.

touchdown scenarios with a margin of 1 ft/s. A touchdown deceleration at a sink rate of 3 ft/s results in an acceleration normal to the vehicle of magnitude 0.35 g. This value is based on a gear stroke length of 5 in. A more conservative design condition of a 4.0-g touchdown will be utilized. These loads exceed those of the nominal or maximum landing sink rate.

Thus, the five design cases are 8-g abort, 8-g abort plus 10 psi overpressure, internal pressurization with 3-g acceleration (ascent), 2.5-g subsonic aerodynamic pullup maneuver, and a 4-g landing. These cases will be analyzed with a methodology as described in the following section.

Analysis Methodology

A finite element modeling and analysis technique is utilized to determine the integrity of the structural arrangement. The ability of the structure to resist local mechanical failure modes and global buckling when subjected to aerodynamic and inertial loading present during the mission is the primary concern. Thus, the analysis includes geometry modeling, finite element modeling, external load generation and application, finite element analysis, structural element sizing, structural element weight summation, and postprocessing results evaluation as noted in Fig. 7.

The geometry concepts are modeled through the use of the SMART (Solid Modeling Aerospace Research Tool) system.[7] The models are stored as bicubic patch data, which are transferred to the finite element and aerodynamics packages. The aerodynamic analysis is performed utilizing a modified Newtonian technique included in the APAS (Aerodynamic Preliminary Analysis System) code[8-9] to predict the pressures which are mapped onto the structural finite element model. The inertial acceleration vectors are calculated utilizing POST[10] (Program to Optimize Simulated Trajectories). The inertial loads output from POST are combined with the aerodynamic loads output from APAS to simulate the critical mission loading conditions.

The structural finite element model is derived in PATRAN[11] by discretizing the SMART geometry surface into a finite element model. Internal structure and additional surface definition are created based on structural engineering experience. Internal structural arrangements may include ring frames, longerons, bulkheads, and truss structures. These structures are incorporated into the vehicle to withstand the external loading and provide safe loading paths which make the vehicle capable of completing the mission without structural failure. The appropriate material properties of the structure are also included in the finite element model of the vehicle.

Finite element analysis (FEA) is performed on the finite element model in order to determine the resulting loads due to the mission loading conditions. Finite element analysis is performed utilizing EAL[12] (Engineering Analysis Language). The FEA produces resultant structural loads for each finite element. These resultant loads are indicative of the load paths

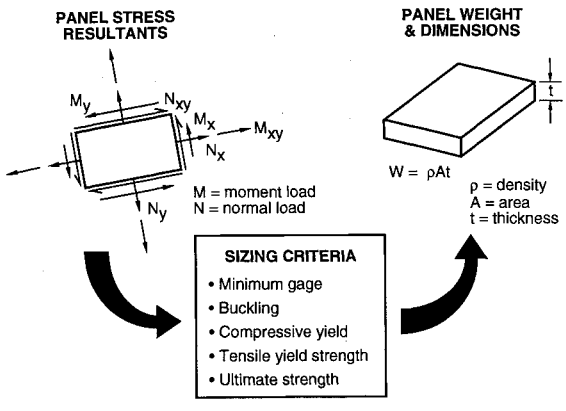

Fig. 8 EZDESIT finite element sizing methodology (flat plate).

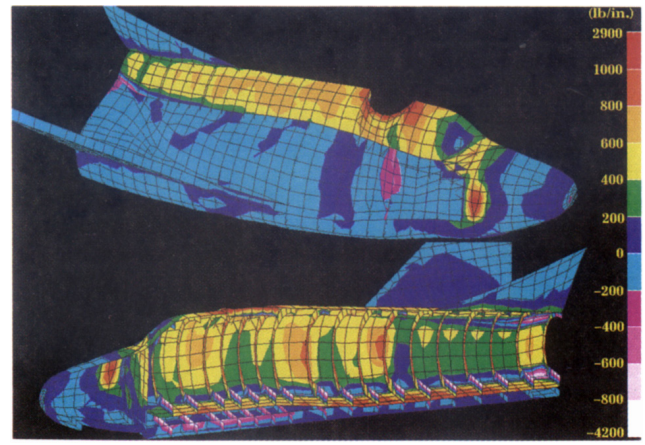

Fig. 9 Ascent conditions, hoop loads.

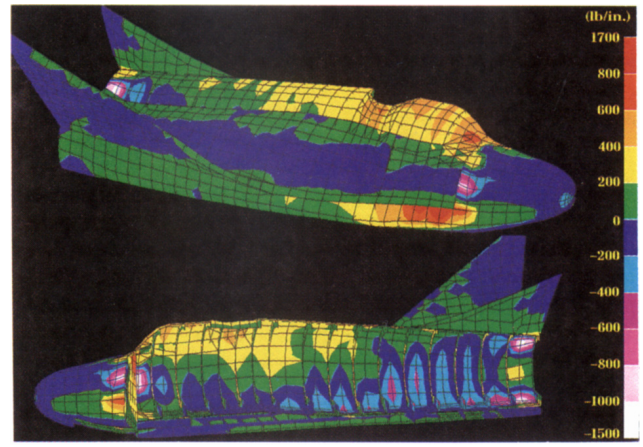

Fig. 10 Ascent conditions, axial loads.

and integrity of the vehicle structure and may indicate areas of the vehicle that are stressed beyond the limits of the construction material. These loads are used as input to a structural sizing routine in order to determine the increases in structural dimensions required to meet or exceed failure criteria. Each structural element (including bars, planar beams, and plate elements) is sized within the EZDESIT program[13] to withstand the mission loading conditions (Fig. 8). The weights of all of the structural finite elements are summed to obtain the total structural weight of the vehicle (HL-20). The geometric sizing of the structural elements alters the stiffness properties of the vehicle finite element model. Thus, the FEA and structural element sizing are iterated until a vehicle weight convergence is achieved. Convergence occurs when the difference between the structural weight of two consecutive iterations is negligible. A converged solution typically takes three iterations. The results of the sizing can be reviewed in two different manners. An interactive session of the EZDESIT program permits the designer to review the data in tabular form. The weight of the HL-20 structure is calculated and displayed by component, load case, failure mode, and element type. In the second method, the EZDESIT results are read into PATRAN (a finite element preprocessor and postprocessor), and the structural element results are graphically displayed on the model. These plots include resultant load paths, dominant load cases, failure modes, and unit weights. Highly loaded areas may indicate a need for an alternative structural design. Resultant loads are reviewed by the structural designer, and if necessary, changes to the structural arrangement are made by altering the finite element model and reanalyzing the structure.

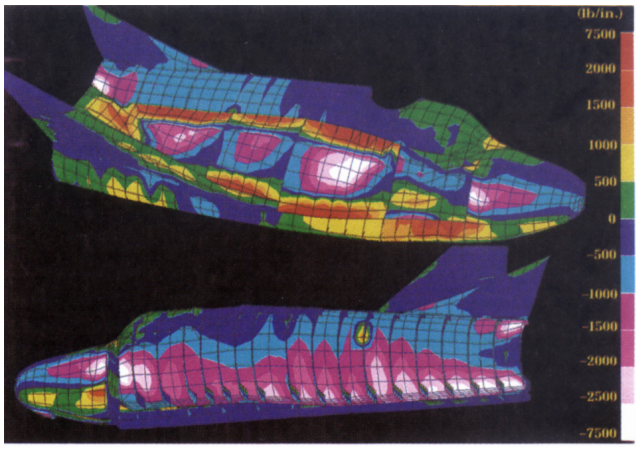

Fig. 11 Abort conditions, hoop loads.

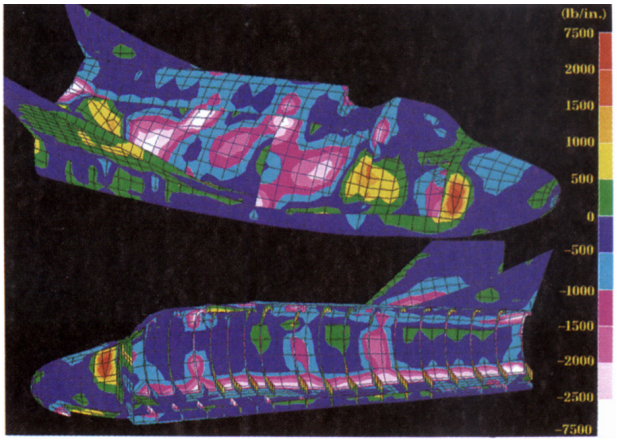

Fig. 12 Abort conditions, axial loads.

Each finite element model is checked for global buckling. The eigensolver routine of EAL is utilized to determine the percent of static loads necessary to obtain a globally buckled model. An eigensolution is performed on the following equation:

$$[K]\{d\} + l[Kg]\{d\} = 0$$

where

K = stiffness matrix
Kg = geometric stiffness matrix
d = displacements
l = eigenvalue

When the eigenvalue is less than one, the loads are too great and global buckling occurs. Thus, an optimum configuration would attain a global buckling eigenvalue of one plus additional margin for the factor of safety.

Results

Resultant loads for the ascent conditions are shown in Figs. 9 and 10. Hoop loading is evident in the crew compartment due to the internal pressurization (Fig. 9). These loads do not transfer to the access doors or the heatshield. Along the flattened floor of the crew compartment, bending moments incur a larger hoop loading. The maximum tensile loading occurs along the aft end of the crew compartment floor with most of the hoop load acting between 200 to 600 lb/in. Axial running loads in the crew compartment (Fig. 10) are compressive. These loads dissipate quickly and are essentially localized loading. These loads dissipate below 400 lb/in. within 4 ft of the aft end of the vehicle.

The 8-g abort plus overpressure condition yields the maximum loading for the mission. Axial loads are shown in Fig. 11. In the pressurized crew compartment, the axial loads reach a maximum of 12600 lb/in. in compression at the aft end of the vehicle and dissipate to less than 500 lb/in. at approximately half the body length. The access panel axial loads are in excess of 2500 lb/in. in compression and 2000 lb/in. in tension. The effect of the external overpressure combined with the access door attachments and the access door radius of curvature results in the spotted loading effect on the doors. The doors achieve high compressive loads in the center leading to a high tensile load at the edges where the attachment points are located. Hoop loads for the 8-g ascent with overpressures loading are shown in Fig. 12. The hoop loads within the crew compartment are for the most part below 500 lb/in. compression with the exception of the crease where the cylinder meets the flattened floor. The higher loads in the crease result from the bending about this crease incurred due to the overpressures. Additional compression loads occur in the crew compartment where the extension frames meet the compartment. The extension frames exert the load from the access panels.

The effect of the runway landing loads on the vehicle is negligible because of their low magnitude compared with those of the abort and internal pressure cases and is therefore not depicted. The runway landing conditions induce localized loads at the landing gear bays and, more specifically, in the bulkheads to which the main strut of each gear is attached. The direct impact of this type of loading is contained within

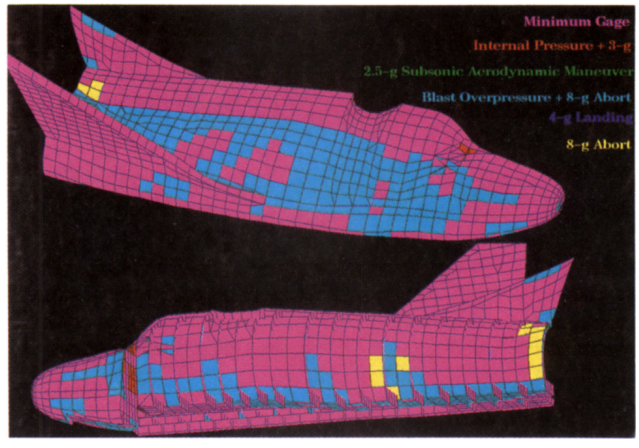

Fig. 13 Critical loading conditions.

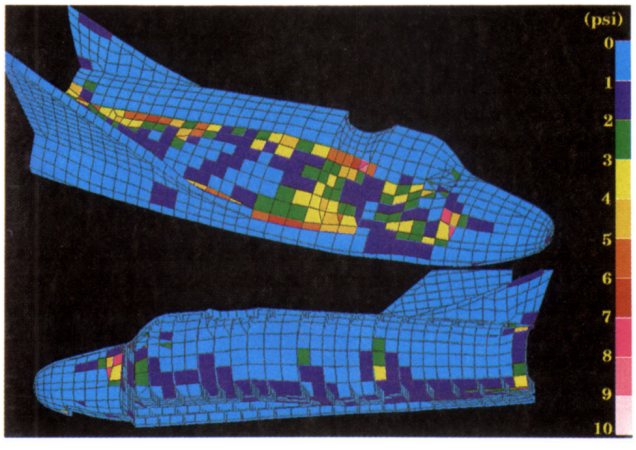

Fig. 14 Panel unit weights.

the bulkheads and extends slightly to the exterior surface surrounding the crew cabin window and has a minimal impact on the overall structural weight.

The effect of the aerodynamic maneuver on the vehicle is primarily that of the wing loading. The result of this loading is not depicted, as it is not a critical condition and does not add significant weight to the vehicle, but is explained here. As expected, the lower surface of the wing is in tension and the upper surface of the wing is in compression due to the aerodynamic loading of the wing. These loads tend to cluster at the leading edge because of the shorter load paths into the body structure. A comparative study of the load cases indicates the wing resultant loads to be greatest for this loading condition. The combination of the wing loads entering the body and the normal acceleration on the body results in a body load map similar to that of the wing loads. The body experiences axial tension in the lower surface and axial compression in the upper surface and these forces are due mainly to the normal acceleration flexing of the structure. Lateral loads in the body are also in tension on the bottom surface and in compression on the top surface. In contrast to the axial loads, these lateral loads are additionally induced by the introduction of wing loads into the body. The unusual intersection angle of the wing and body introduces a canted load path in the body. These paths can be critical because of the abrupt change of curvatures found on the body surface. Aerodynamic loads deflect the wing upward, placing a moment load at the wing/body intersection. This moment is evident in the lateral loads of the body. The wing deflection places a compressive load into the upper skin and a tensile load into the lower skin. The ring frames and the bulkhead of the body act to carry the load through the body, as exhibited in the high load levels. Thus, both the wing and parts of the body are critically loaded by the aerodynamic maneuver.

Resultant loads are used as input to a structural sizing failure analysis. Physical properties of each element are sized to withstand an array of structural failure criteria and the exact details of this operation are found in the Analysis Methodology section of this paper. A weight for each sized element results from this sizing operation. The critical loading condition for each individual panel can be determined and is displayed in Fig. 13. As shown in the figure, minimum gauge panels are sufficient for most of the HL-20 structure, comprising 1530 lb of the total 2480 lb. The remainder of the structure is sized almost entirely by the abort condition, 880 lb. While the other cases contribute only 50 lb, the buckling condition adds an extra 70 lb. These values do not include the weight of the crew-compartment window, seats, or the hatches. The structural weight (2480 lb) of the vehicle is approximately 13% of the total dry weight (19,450 lb) of the vehicle. A graphical representation of the vehicle unit weights by element is presented in Fig. 14. In this figure, the effect of the abort blast overpressures on the doors is evident. The doors are attached to the rest of the structure at only a few points, thus the external loads are not easily transferred into the rest of the structure, leading to a thicker construction and higher unit weight. The average unit weight for the structure, including the weight for longerons and bars, is 1.34 lb/ft^2. These values were obtained by applying a 1.5 non-optimum factor to all conditions during the analysis phase.

Concluding Remarks

A preliminary structural configuration for the HL-20 has been designed to successfully fulfill the loading requirements of the mission. The loading conditions include ascent conditions, a subsonic aerodynamic maneuver, a landing condition, and abort and an abort with blast overpressures. The configuration was analyzed for the loading conditions through a finite element technique and panel sizing routine. The structure satisfies the various loading conditions which evolved from the HL-20 reference mission. Finite elements representing structure were sized individually to meet the mission requirements and result in a vehicle structural weight of about 2500 lb. The structural weight is approximately 10% of the estimated total weight of the HL-20 vehicle. Thus, the structure meets the performance requirements of the vehicle.

Minimum-gauge constraints size 61% of the structure. An abort scenario with blast overpressures sizes 36% of the structure and the remaining 3% of the structure weight is sized by the other mission loading conditions and global buckling. The current structural configuration satisfies all of the loading requirements; however, further studies should be performed to refine the structural configuration for reduced loads and decreased weight. For further studies, particular attention should be focused on the design of the access doors, which carry a significant amount of loading and are consequently high in unit weight.

References

[1]Bush, L. B., Lentz, C. A., Robinson, J. A., and MacConochie, I. O., "Structural Design Considerations for a Personnel Launch System," *Journal of Spacecraft and Rockets,* Vol. 29, No. 1, 1992, pp. 138–149.

[2]Ehrlich, C., "HL-20 Concept: Design Rationale and Approach," *Journal of Spacecraft and Rockets,* Vol. 30, No. 5, 1993, pp. 573–581.

[3]Willshire, K. F., Simonsen, L. C., and Willshire, W. L., "Human Factors Evaluation of the HL-20 Full Scale Model," *Journal of Spacecraft and Rockets,* Vol. 30, No. 5, 1993, pp. 606–614.

[4]Stubbs, S., "Landing Characteristics of a Dynamic Model of the HL-10 Manned Lifting Entry Vehicle," NASA TN D-3570, Nov. 1966.

[5]Naftel, J. C., Powell, R. W., and Talay, T. A., "Performance Assessment of a Space Station Rescue and Personnel/Logistics Vehicle," *Journal of Spacecraft and Rockets,* Vol. 27, No. 1, 1990, pp. 76–81.

[6]Cruz, C. I., Ware, G. M., Grafton, S. B., Woods, W. C., and Young, J. C., "Aerodynamic Characteristics of a Proposed Personnel Launch System (PLS) Lifting-Body Configuration at Mach Numbers From 0.05 to 20.3," NASA TM-101641, Nov. 1989.

[7]McMillan, M. L., Rehder, J. J., Wilhite, A. W., Schwing, J. L., and Mills, J. C., "A Solid Modeler for Aerospace Vehicle Preliminary Design," AIAA Paper 87-2901, Sept. 1987.

[8]Bonner, E., Clever, W., and Dunn, K., "Aerodynamic Preliminary Analysis System II, Part I—Theory," Rockwell International Corp., NASA CR-182076, April 1991.

[9]Sova, G., and Divan, P., "Aerodynamic Preliminary Analysis System II, Part II—User's Manual," Rockwell International Corp., NASA CR-182077, April 1991.

[10]Brauer, G. L., Cornick, D. E., Olson, D. W., Petersen, F. M., and Stevenson, R., "Program to Optimize Simulated Trajectories (POST), Vol. II," Martin Marietta Corp., MCR-87-583, Denver, CO, Sept. 1987.

[11]Anon., "PATRAN Plus User's Manual," PDA Engineering, Release 2.3 Publication No. 2191020, Costa Mesa, CA, July 1988.

[12]Whetstone, W. D., "Engineering Analysis Language Reference Manual," Engineering Information Systems, Inc., San Jose, CA, July 1983.

[13]Cerro, J. A., and Shore, C. P., "EZDESIT, A Computer Program for Structural Element Sizing and Vehicle Weight Prediction," NASP CR-1092, July 1990.